Polyhedron 158 (2019) 325–333

Contents lists available at ScienceDirect

Polyhedron

journal homepage: www.elsevier.com/locate/poly

Platinum complexes containing or derived from olefinic phosphines $P(X)((CH_2)_6CH{=}CH_2)_2$ (X = OH, Ph, $(CH_2)_6CH{=}CH_2$); ring closing metatheses, structures, and *trans*/*cis* isomerizations

Michael Stollenz [1,2], Hemant Joshi [3], Andreas Ehnbom [4], Tobias Fiedler [5], Sugam Kharel [6], Joseph H. Reibenspies, Nattamai Bhuvanesh, Michael B. Hall [7], John A. Gladysz *,[8]

Department of Chemistry, Texas A&M University, PO Box 30012, College Station, TX 77842-3012, USA

ARTICLE INFO

Article history:
Received 8 August 2018
Accepted 14 September 2018
Available online 25 September 2018

"To William D. Jones, in appreciation of his many fundamental contributions to organometallic chemistry and exemplary qualities as a colleague."

Keywords:
Alkene metathesis
Trans/*cis* isomerization
Hydrogen bonding
DFT calculations
Platinum

ABSTRACT

The reaction of $(O{=})PH((CH_2)_6CH{=}CH_2)_2$ (2.0 equiv) and $PtCl_2$ in toluene gives *trans*-$PtCl_2(P(OH)((CH_2)_6CH{=}CH_2)_2)_2$ in 68% yield as a 82:18 mixture of Pt–Cl···H–OP hydrogen bond isomers. Addition of Grubbs' first generation catalyst followed by hydrogenation (5 bar, cat. $RhCl(PPh_3)_3$ or PtO_2) affords the doubly *trans* spanning macrocyclic diphosphine adduct *trans*-$[PtCl_2(P(OH)((CH_2)_{14})_2P(OH))$ (31–9% crude yields). A crystal structure shows that the two OH groups are *anti*, and hydrogen bond to opposite Cl–Pt–Cl chlorine atoms. The reaction of $P(Ph)((CH_2)_6CH{=}CH_2)_2$ (2.0 equiv) and $PtCl_2$ in toluene gives *cis*-$PtCl_2(P(Ph)((CH_2)_6CH{=}CH_2)_2)_2$ (*cis*-**5**, 40%) and *trans*-**5** (8%). The crystal structure of the former is determined. The *trans*/*cis* equilibrium ratios of these and related complexes are probed by DFT. Attempts to crystallize *trans*-$PtCl_2((H_2C)_{14}P((CH_2)_{14})P(CH_2)_{14})$ (*trans*-**7′**), which is a minor product from a published metathesis/hydrogenation sequence involving *trans*-$PtCl_2(P((CH_2)_6CH{=}CH_2)_3)_2$, give only *cis*-**7′**, as established by ^{31}P NMR and crystallography.

© 2018 Elsevier Ltd. All rights reserved.

1. Introduction

The application of alkene metatheses in metal coordination spheres, using C=C linkages present in pendant ligands, can lead to unprecedented molecular architectures [1–8]. One of our interests has involved metal complexes that feature sterically shielded ML_y rotators, as exemplified by **II** [3], **IV** [4], **VII** [5–8], and **VIII** [6,8] in Scheme 1. Species of the type **VII** are thought to have particular promise as molecular gyroscopes [9–11]. Towards these and other ends, we have studied the metatheses of a plethora of bis(phosphine) complexes with $P(CH_2)_mCH{=}CH_2$ moieties (e.g., **I**, **III**, **VI**), especially for $m = 6$. Only systems with *trans* P–M–P linkages are depicted in Scheme 1, but the corresponding *cis* isomers [12] as well as similar As–M–As [5c] and Se–M–Se [4c] adducts are also of interest.

During the course of this work, a few nuggets have been lost in the shuffle, e.g. excluded from already long full papers for reasons such as peer/editorial input, streamlining, timing, or partial characterization. In this paper, we describe several related themes that have come to somewhat later fruition, but provide substantive advances and/or added support for previously proposed structure/property correlations. The most interesting of these suggests a new approach to modulating rotational barriers in species of the type **IV** by introducing functionality into the phosphorus substituents X that can interact with the rotator.

2. Results

2.1. $P(OH)((CH_2)_6CH{=}CH_2)_2$ systems

The secondary dialkylphosphine oxide $(O{=})PH((CH_2)_6CH{=}CH_2)_2$ (**1**) has been isolated in 79% yield from the reaction of commercial diethyl phosphonate, $(O{=})PH(OCH_2CH_3)_2$, and a three

* Corresponding author.
E-mail address: gladysz@mail.chem.tamu.edu (J.A. Gladysz).
[1] Current address: Department of Chemistry and Biochemistry, Kennesaw State University, 370 Paulding Building NW, MD#1203, Kennesaw, Georgia 30144, USA.
[2] ORCID: 0000-0002-8635-164X.
[3] ORCID: 0000-0002-7616-0241.
[4] ORCID: 0000-0002-7044-1712.
[5] ORCID: 0000-0001-7169-305X.
[6] ORCID: 0000-0001-6106-4639.
[7] ORCID: 0000-0003-3263-3219.
[8] ORCID: 0000-0002-7012-4872.

https://doi.org/10.1016/j.poly.2018.09.025
0277-5387/© 2018 Elsevier Ltd. All rights reserved.

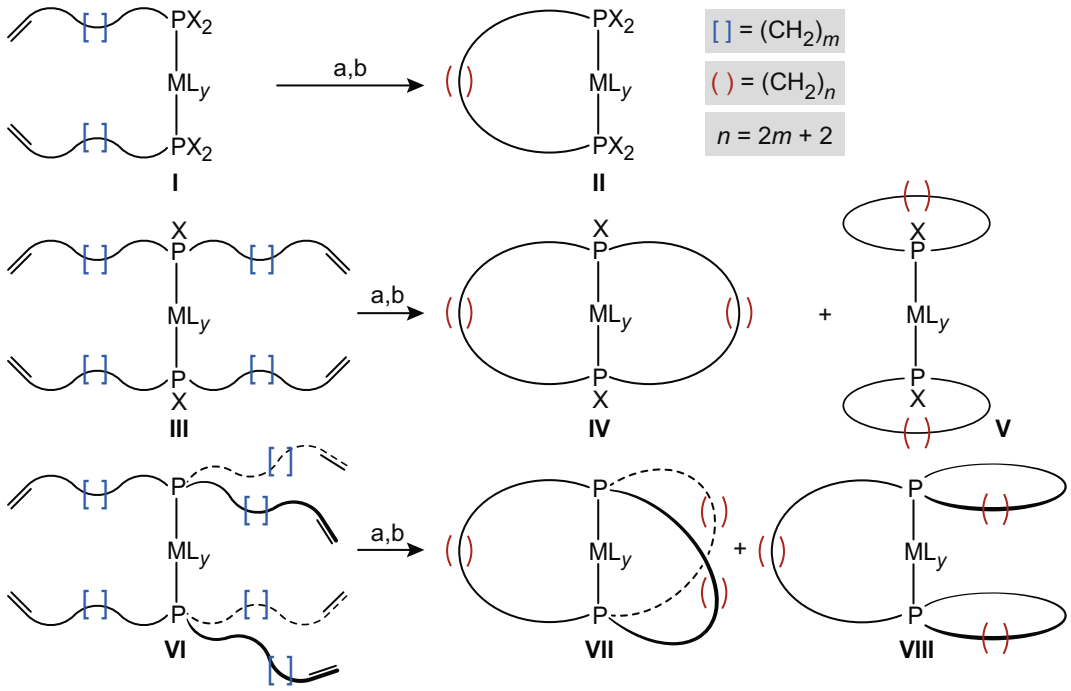

Scheme 1. Routes to sterically shielded ML_y rotors: (a) alkene metathesis; (b) hydrogenation.

fold excess of the Grignard reagent $BrMg(CH_2)_6CH{=}CH_2$ [13]. For both the starting material and product, the tautomeric structures with trivalent phosphorus atoms, HO-PX_2 – termed phosphinous acids when X = R or Ar – are much less stable [14]. Nonetheless, they are often preferentially sequestered by transition metals and have an extensive coordination chemistry [15].

As shown in Scheme 2, **1** (2.0 equiv) and $PtCl_2$ were combined in toluene at room temperature. Such procedures often give easily separable mixtures of *trans*/*cis* $PtCl_2L_2$ adducts that can be distinguished by the magnitudes of the $^1J_{PPt}$ values (*trans* << *cis*) [16]. In the case of *trialkyl*phosphines, *cis* isomers dominate in more polar solvents and *trans* isomers in less polar solvents [17,18], although steric effects can also come into play. Accordingly, a chromatographic workup gave the oily bis(phosphinous acid) complex *trans*-$PtCl_2(P(OH)((CH_2)_6CH{=}CH_2)_2)_2$ (*trans*-**2**) in 68% yield, which was characterized by NMR (^{1}H, ^{13}C{^{1}H}, ^{31}P{^{1}H}) as summarized in the experimental section and depicted in the Supporting information.

A variety of platinum(II) complexes of phosphinous acids have been reported [15,19–21], as further detailed in the discussion section. The NMR properties of *trans*-**2** closely mirrored those of the bis(*t*-butyl) analog *trans*-$PtCl_2(P(OH)(t\text{-}Bu)_2)_2$ [20], particularly with respect to a doubled set of ^{13}C{^{1}H} and ^{31}P{^{1}H} signals that indicated a ca. 82:18 mixture of two *trans* isomers ($^1J_{PPt}$ = 2387/2391 Hz). These were assigned, as in the earlier study [20], to *anti* and *syn* hydrogen bonding motifs as depicted in Scheme 2.

Next, dilute CH_2Cl_2 solutions of *trans*-**2** (0.0035–0.00082 M) and CH_2Cl_2 solutions of Grubbs' first generation catalyst (3.1–6.6 mol%) were combined. After 39–48 h, the crude products were treated with H_2 in the presence of Wilkinson's catalyst, $RhCl(PPh_3)_3$ (25 mol%, 38 °C), or PtO_2 (17 mol%, 50 °C). After 18–48 h, column chromatography gave the target complex *trans*-$\overline{PtCl_2(P(OH)((CH_2)_{14})_2P(OH))}$ (*trans*-**3**) in 31–9% crude yields from *trans*-**2**. The ^{31}P{^{1}H} NMR spectra showed $^1J_{PPt}$ values of 2471–2473 Hz, as well as some minor components (17–21% total) for which ^{195}Pt satellites could not be resolved. One possible byproduct would feature an alternative disposition of the P—OH hydroxy groups (*vide infra*).

Single crystals of *trans*-**3** were obtained from CH_2Cl_2/diethyl ether. The structure was determined by X-ray diffraction as summarized in Table 1 and the experimental section. The OH hydrogen atoms were located from an electron density map, and the platinum atom was coincident with an inversion center. The molecular structure is depicted in Fig. 1, and key bond lengths and angles are given in the caption. The P—OH groups feature an *anti* as opposed to a *syn* orientation, as illustrated in **X** and **XI** in Scheme 3 and reflected by a O—P—P—O torsion angle of 180.0°. Furthermore, both OH hydrogen atoms engage in hydrogen bonding to opposite chloride ligands, as reflected by OH···Cl and O···Cl distances of 2.333 Å and 3.078 Å, and P—O—H, O—H—Cl, H—Cl—Pt, and O—P—Pt—Cl angles of 112.9°, 139.0°, 84.0°, and 3.1°. The IR spectrum showed a broad ν_{PO-H} band at 3302 cm^{-1}.

2.2. Other $P(X)((CH_2)_6CH{=}CH_2)_2$ systems

The tertiary monophenyl phosphine $P(Ph)((CH_2)_6CH{=}CH_2)_2$ (**4**) can be prepared from $PhPCl_2$ and $BrMg(CH_2)_6CH{=}CH_2$ (2.0 equiv) in 90% yield [4b] or $PhPH_2$, *n*-BuLi (2.0–2.1 equiv), and $Br(CH_2)_6$-$CH{=}CH_2$ (2.0–2.1 equiv) in 78% yield [4a]. The first procedure scales somewhat better. Thus, **4** and $PtCl_2$ were combined in toluene (2:1 mol ratio). The conditions were analogous to those used with **1** in Scheme 2. As shown in Scheme 4 (top), a chromatographic workup (CH_2Cl_2) gave $PtCl_2(P(Ph)((CH_2)_6CH{=}CH_2)_2)_2$ (**5**). However, now the major product was *cis*-**5**, obtained as a colorless solid in 40% yield ($^1J_{PPt}$ 3550 Hz); *trans*-**5** was isolated as a yellow oil in 8% yield ($^1J_{PPt}$ 2462 Hz) that usually contained minor amounts (ca. 10%) of *cis*-**5**. A ^{31}P{^{1}H} NMR spectrum of the reaction mixture prior to chromatography showed a 82:18 *trans*/*cis* mixture. When hexanes was added to solidified samples, only the less polar *trans*-**5** was extracted. The *trans*/*cis* equilibrium was further probed computationally as described in Section 2.3 below.

Crystals of *cis*-**5** could be grown by the slow evaporative concentration of diethyl ether solutions. The X-ray structure was

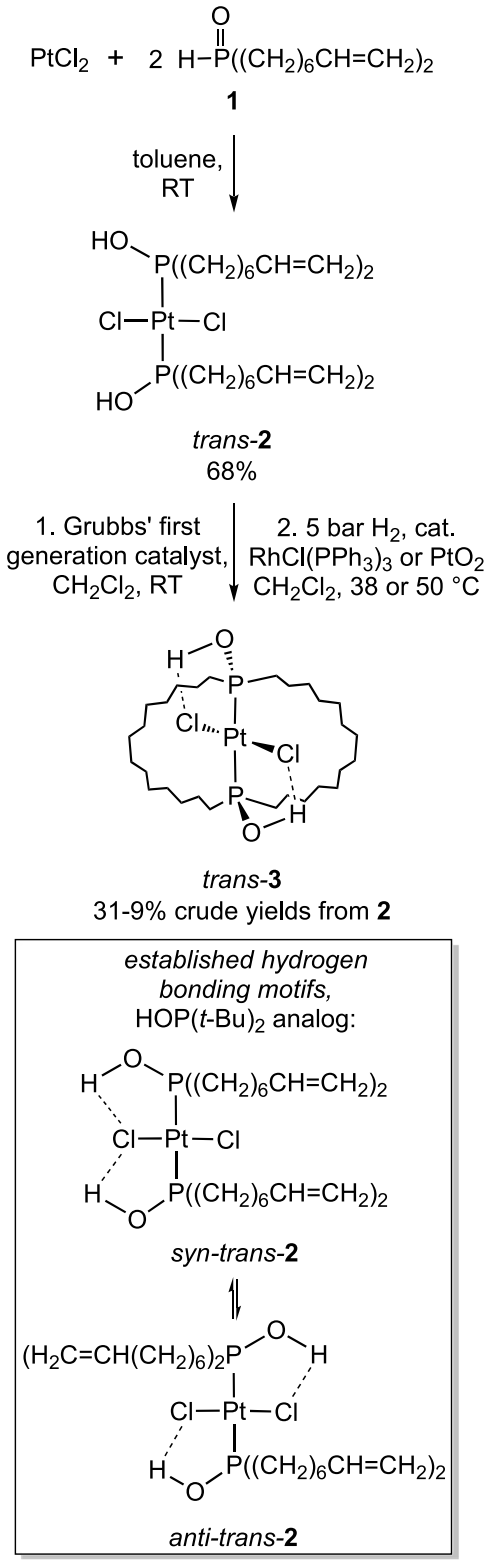

Scheme 2. Syntheses of new platinum complexes containing $P(OH)R_2$ ligands.

solved analogously to that of *trans*-**3**, and the molecular structure is depicted in Fig. 2 (top), together with key bond lengths and angles (caption). One eight carbon segment was disordered (C1_5 to C8_5), but this could be modeled as described in the experimental section. The dominant conformation is depicted in Fig. 2.

Additional *trans*/*cis* isomerization phenomena were noted with other platinum complexes. As shown in Scheme 4 (bottom), the conversion of *trans*-$PtCl_2(P((CH_2)_6CH{=}CH_2)_3)_2$ (*trans*-**6**), akin to **VI** in Scheme 1, to the gyroscope like complex *trans*-$PtCl_2(P((CH_2)_{14})_3P)$ (*trans*-**7**) and the isomer *trans*-$PtCl_2((H_2C)_{14}P((CH_2)_{14})P(CH_2)_{14})$ (*trans*-**7′**) has been described earlier [6a,b]. Complexes of the latter type, which are derived from a combination of *intra*ligand and *inter*ligand metathesis, have proved much more difficult to crystallize [6c,8a]. Thus, attempts were made to grow crystals of *trans*-**7′** by the evaporative concentration of diethyl ether solutions.

Some tiny colorless plates formed over the course of several months. The $^{13}C\{^1H\}$ NMR spectrum of the accompanying bright yellow oil showed only *trans*-**7′**. However, an X-ray structure (Fig. 2, bottom) indicated that *cis*-**7′** had crystallized. A $^{31}P\{^1H\}$ NMR spectrum of a $CDCl_3$ solution of the crystals gave a $^1J_{PPt}$ value (3522 Hz) diagnostic of *cis* stereochemistry. Curiously, two higher homologs with rings containing twenty and twenty two methylene groups (**8′** and **9′** in Scheme 5, top) crystallized in the same manner – i.e. small amounts of a crystalline *cis* complex from a *trans* precursor after extended periods of time [6c]. Hence, there must be kinetic or thermodynamic obstacles associated with assembling crystal lattices from *trans*-**7′**–**9′** alone.

As shown in **XIII** in Scheme 5 (bottom), when the structure of *cis*-**7′** is viewed down the phosphorus–phosphorus vector, the phosphorus–carbon bonds appear eclipsed. The corresponding C—P—P—C torsion angles fall into the narrow range of 1.3–3.1°. As illustrated in Fig. 2 (bottom), the two macrocycles derived from *intra*ligand metatheses are stacked on top of each other, a feature also found in the structures of the higher homologs *cis*-**8′** and *cis*-**9′** (Scheme 5) [6c].

2.3. Computational analysis of trans/cis equilibria

We sought insight as to why *cis*-**5** dominated in Scheme 4 when under analogous conditions (toluene solvent) trialkylphosphine ligands afforded mainly *trans*-$PtCl_2L_2$ adducts [17,18]. Could a single phenyl substituent account for this difference? Thus, DFT calculations were carried out as described in the experimental section for *trans* and *cis* complexes with ligands of the formula $P(Ph)_z((CH_2)_6CH{=}CH_2)_{3-z}$ ($z = 0$–3).

As shown in Fig. 3, the isomerization of *trans*- to *cis*-$PtCl_2(P((CH_2)_6CH{=}CH_2)_3)_2$ ($z = 0$) was computed to be markedly downhill in CH_2Cl_2 (−5.2 kcal/mol), and roughly thermoneutral in toluene or the gas phase, reproducing the preparative trend for trialkylphosphine ligands. Importantly, with the monophenyl substituted phosphine ligand, the isomerization of *trans*- to *cis*-$PtCl_2(P(Ph)((CH_2)_6CH{=}CH_2)_2)_2$ was markedly downhill in CH_2Cl_2 *and* in toluene *and* in the gas phase (−7.0 to −3.7 kcal/mol), in accord with the preparative data for **5** in Scheme 4.

This trend continued with the diphenyl substituted phosphine ligand, with the isomerization of *trans*- to *cis*-$PtCl_2(P(Ph)_2((CH_2)_6CH{=}CH_2))_2$ even further downhill (−13.4 to −11.8 kcal/ mol). For the corresponding triphenylphosphine complex $PtCl_2(PPh_3)_2$ ($z = 3$), *trans* to *cis* isomerization remained downhill, but the energy differences were intermediate between the ranges for $z = 1$ and 2 (−11.6 to −6.2 kcal/mol), suggesting counteracting contributing factors as outlined in the discussion section. In any case, there are abundant experimental data supporting the greater thermodynamic stability of *cis*-$PtCl_2(PPh_3)_2$ in a variety of media [22].

3. Discussion

As noted above, a number of platinum(II) complexes of phosphinous acid ligands have been synthesized [15,19–21], and those of the formula $PtCl_2(P(OH)R_2)_2$ are the most relevant to Scheme 2. An extensive series of *trans* and *cis* isomers has been reported by

Table 1
Summary of crystallographic data.

	trans-**3**	*cis*-**5**	*cis*-**7′**
Empirical formula	$C_{28}H_{58}O_2P_2PtCl_2$	$C_{44}H_{70}P_2PtCl_2$	$C_{42}H_{84}P_2PtCl_2$
Formula weight	754.67	926.93	917.02
Temperature [*K*]	110(2)	110(2)	110(2)
Diffractometer	Bruker GADDS	Bruker GADDS	Bruker GADDS
Wavelength [*Å*]	1.54178	1.54178	1.54178
Crystal system	monoclinic	monoclinic	monoclinic
Space group	*P* $2_1/n$	*P* $2_1/c$	*P* $2_1/n$
Unit cell dimensions			
a [Å]	9.478(5)	16.377(9)	17.6893(12)
b [Å]	11.400(5)	9.823(5)	13.6561(9)
c [Å]	15.612(5)	28.290(14)	20.0334(17)
α [°]	90.00	90.00	90.00
β [°]	102.988(5)	98.89(2)	113.573(4)
γ [°]	90.00	90.00	90.00
V [$Å^3$]	1643.7(12)	4496(4)	4435.6(6)
Z	2	4	4
ρ_{calc} [Mg/m^3]	1.525	1.369	1.373
μ [mm^{-1}]	4.551	7.797	7.888
F(0 0 0)	768	1904	1912
Crystal size [mm]	0.10 × 0.05 × 0.05	0.10 × 0.10 × 0.01	0.02 × 0.02 × 0.01
Θ limit [°]	4.85 to 59.97	3.16 to 59.99	2.82 to 55.00
Index range (*h*, *k*, *l*)	−10, 10; −12, 12; −17, 17	−18, 18; −10, 11; −31, 31	−18, 18; −14, 12; −20, 20
Reflections collected	14524	31387	39125
Independent reflections	2417	6499	5382
R_{int}	0.0449	0.1490	0.118
Completeness to Θ	98.2	97.4	96.5
Maximum and minimum transmission	0.8044 and 0.6590	0.9261 and 0.5094	0.3766 and 0.1870
Data/restraints/parameters	2504/0/160	6499/358/475	5382/379/424
Goodness-of-fit (GOF) on F^2	0.990	1.004	1.100
R indices (final) [$I > 2\sigma(I)$]			
R_1	0.0229	0.0506	0.1049
wR_1	0.0587	0.0879	0.2561
R indices (all data)			
R_2	0.0269	0.1038	0.1274
wR_2	0.0596	0.0953	0.2786
Largest difference in peak/hole [e $Å^{-3}$]	0.73 and −0.82	0.799 and −1.094	10.857 and −2.503

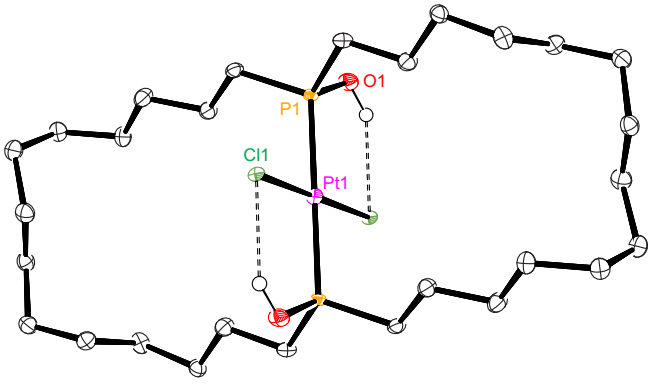

Fig. 1. Thermal ellipsoid plot (50% probability) of *trans*-**3**. Key bond lengths (Å) and angles (°): Pt(1)–P(1) 2.2930(16), Pt(1)–Cl(1) 2.3298(10), P(1)–O(1) 1.621(3), O(1)···Cl(1) 3.078(4), H(1)···Cl(1) 2.333(1), P(1)–Pt(1)–P(1′) 180.00(5), P(1)–Pt(1)–Cl(1) 88.71(4), P(1′)–Pt(1)–Cl(1) 91.29(4), Cl(1)–Pt(1)–Cl(1′) 180.00(5), Pt(1)–P(1)–O(1) 112.35(12), O(1)–H(1)–Cl(1) 139.0(1).

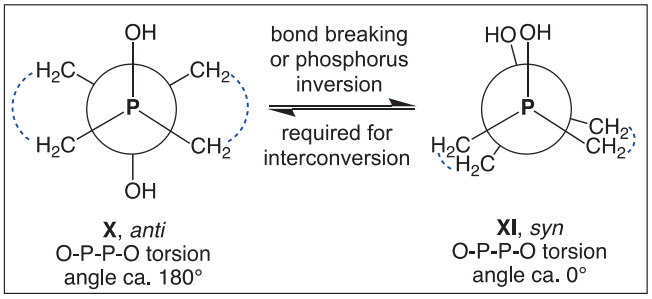

Scheme 3. Representations of the *anti* and *syn* OH diastereomers of *trans*-**3** (the Cl–Pt–Cl moiety is not depicted).

Giordano and Buono (R = *t*-Bu, Cy, Ph, Me, *i*-Bu) [20]. The complexes *trans*-$PtCl_2(P(OH)(t\text{-}Bu)_2)_2$ and *trans*-$PtCl_2(P(OH)(Cy)_2)_2$ crystallize with hydrogen bonding motifs analogous to that of *trans*-**3** (Fig. 1). Both O—P—P—O torsion angles are 180.0°, indicating an *anti* disposition of P–OH groups. The OH···Cl and O···Cl distances (2.309–2.231 Å and 3.008–2.944 Å) and O—H—Cl and O—P—Pt—Cl angles (143.4–145.6° and 9.0–10.3°) are very close to those of *trans*-**3**. As illustrated in Scheme 3, the chelating diphosphinous acid ligand precludes *trans*-**3** from adopting the *syn* hydrogen bonding motif observed for some of these complexes in solution (Scheme 2, bottom).

Interestingly, Hoge has crystallized a similar *trans* bis(phosphinous acid) complex, but with two electronegative aryl substituents of the formula 2,4-$C_6H_3(CF_3)_2$ [19]. Although the P—OH groups are *anti* (O—P—P—O torsion angle 180.0°), the Cl—Pt—Cl vector is not optimally oriented for hydrogen bonding, as reflected by the O—P—Pt—Cl torsion angle of 38.2° (vs. 3.1° for *trans*-**3**). Accordingly, the OH···Cl distance is much longer (3.160 Å), indicative of a substantially weaker interaction, if any. Two related structures with monoaryl phosphinous acids (P(OH)RAr) have also been reported [21]. Although not depicted in any of the published graphics, the metrical parameters suggest some hydrogen bonding (*anti* motif; O—P—P—O and O—P—Pt-Cl torsion angles 157.9–180.0° and 12.4–9.1°; OH···Cl 2.307–2.409 Å; O···Cl 2.981–3.006 Å).

In the preceding studies, only Giordano and Buono reported IR data [20]. In KBr, their two crystallographically characterized

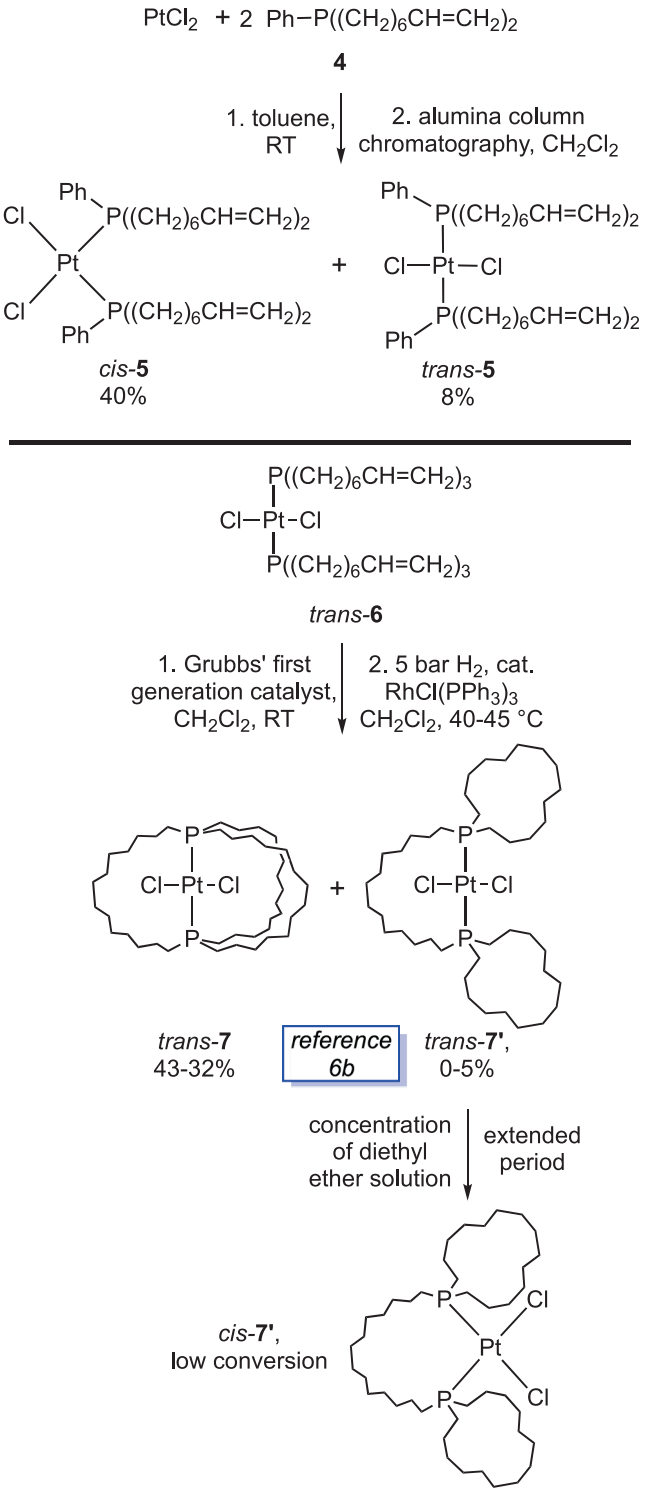

Scheme 4. Syntheses of new platinum complexes containing $P(Ph)R_2$ or other ligands.

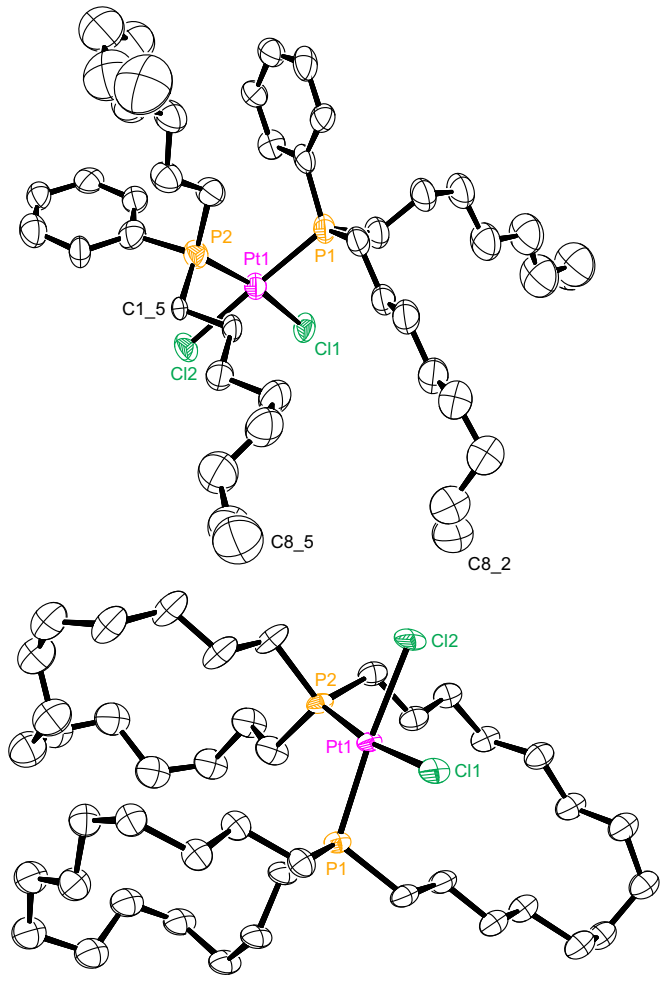

Fig. 2. Thermal ellipsoid plot (50% probability) of *cis*-**5** (top, dominant conformation) and *cis*-**7′** (bottom). Key bond lengths (Å) and angles (°): *cis*-**5** Pt(1)–P(1) 2.260 (2), Pt(1)–P(2) 2.251(2), Pt(1)–Cl(1) 2.350(2), Pt(1)–Cl(2) 2.366(2), P(1)–Pt(1)–P(2) 97.68(9), P(1)–Pt(1)–Cl(1) 91.21(9), P(1)–Pt(1)–Cl(2) 178.53(9), P(2)–Pt(1)–Cl(1) 171.08(8), P(2)–Pt(1)–Cl(2) 83.42(9), Cl(1)–Pt(1)–Cl(2) 87.68(9); *cis*-**7′** Pt(1)-P(1) 2.255(5), Pt(1)-P(2) 2.256(5), Pt(1)-Cl(1) 2.365(5), Pt(1)-Cl(2) 2.359(5), P(1)–Pt(1)–P(2) 104.8(2), P(1)–Pt(1)–Cl(1) 83.85(18), P(1)–Pt(1)–Cl(2) 171.26(18), P(2)–Pt(1)–Cl(1) 171.24(19), P(2)–Pt(1)–Cl(2) 83.84(18), Cl(2)–Pt(1)–Cl(1) 87.54(17).

complexes (*vide supra*) exhibited $\nu_{PO\text{-}H}$ values of 3221–3258 cm^{-1}, quite close to the 3302 cm^{-1} found for *trans*-**3** (ATR, powder film).

The rotation of the Cl—Pt—Cl moiety in gyroscope like complexes such as *trans*-**7** (Scheme 4) remains fast on the NMR time scale, even in $CDFCl_2$ at −120 °C [6b]. An appropriately placed hydroxy group represents a possible way to modulate these rotational barriers, in particular rendering them higher and easier to quantify by standard variable temperature NMR techniques. However, *trans*-**3** also has too high a symmetry to probe Cl—Pt—Cl rotation by NMR. One of several modifications that might yield a tractable system would involve replacing one of the hydroxy groups by an alkyl substituent, and both of the chloride ligands by magnetically active fluoride ligands. The most likely ground state would now show two ^{19}F signals. A related possibility would involve a diastereomer with *syn* P-OH groups and fluoride ligands.

There is an obvious conceptual relationship between *trans*-**3** and the bis(dialkylselenide) complexes **10a**,**b** shown in Scheme 6. These crystallize with the selenium lone pairs *anti*. NMR data show that the selenium atoms undergo facile pyramidal inversion in solution, and the *anti* isomers are believed to be more stable. In contrast, the corresponding bis(phenylphosphine) complexes (i.e., **IV** with X = Ph in Scheme 1) lack low energy pathways by which the phosphorus stereocenters can equilibrate. For all systems studied to date, isomers with *syn* phenyl groups dominate kinetically [4a]. Rationales have been proposed [4a,c]. Presumably the P-OH groups in *trans*-**2** direct, through hydrogen bonding, the formation of the *anti* isomer of *trans*-**3**. A possible assembly is shown in **XIV** in Scheme 5 (bottom).

The *trans*/*cis* selectivity associated with **5** in Scheme 4 is opposite those of bis(*trialkyl*phosphine) platinum dichloride complexes prepared in benzene or toluene [17–18]. This dichotomy is also

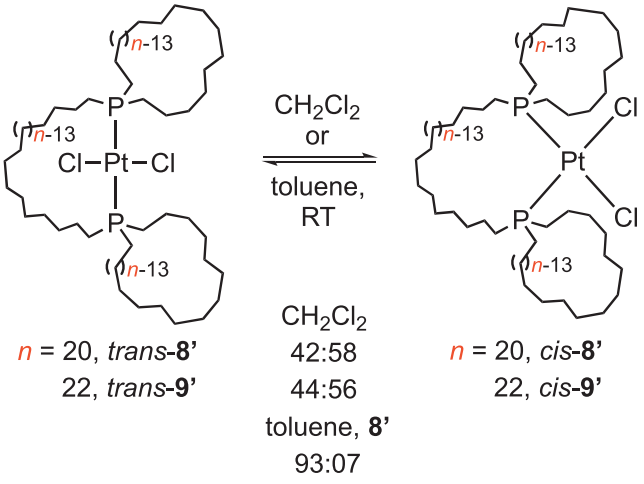

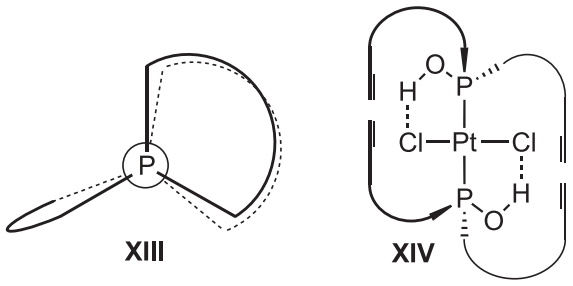

Scheme 5. Other relevant complexes, equilibria, and structures.

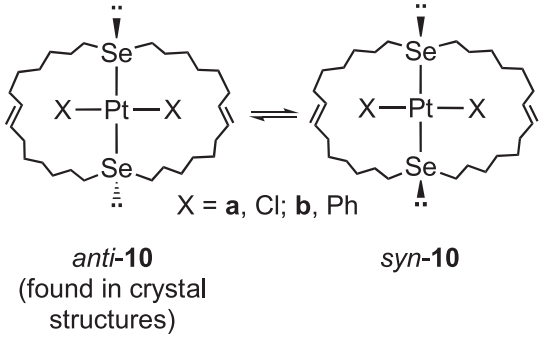

Scheme 6. Doubly *trans*-spanning bis(dialkyl selenide) complexes.

illustrated by the equilibria for **8**′ and **9**′ in Scheme 5 (top), which are heavily biased towards *trans* isomers in toluene and moderately biased towards *cis* isomers in CH_2Cl_2 [6b]. DFT calculations (gas phase) nicely reproduce the trends in toluene [12b]. It is well established that replacing alkyl phosphine substituents by phenyl groups enhances π acceptor strengths [23]. Thus, the most economical rationalization for the experimental data would be that the proportion of *cis* isomer increases as the π acceptor strength of the phosphorus donor ligands increases. This places the moderately π donating chloride ligands *trans* to the phosphorus donor ligands that rank higher in π acidity.

Indeed, as noted in two companion papers [12], only *cis* analogs of **VI** (Scheme 1, $ML_y = PtCl_2$) can be accessed in the case of trialkylphos*phites*, which are generally stronger π acceptors than trialkyl and triarylphosphines [23]. However, the fact that the *trans* to *cis* isomerization of $PtCl_2(PPh_3)_2$ is not computed to be as favorable as with $PtCl_2(P(Ph)_2((CH_2)_6CH{=}CH_2))_2$ (Fig. 3) indicates that there is another factor at work, at least in this series of compounds. Although further analysis is beyond the scope of this study, steric effects associated with the greater number of phenyl groups, the loss of van der Waals interactions associated with the $(CH_2)_6CH{=}CH_2$ groups, and edge/face phenyl/phenyl interactions [24] represent possibilities. Surprisingly, there does not seem to be a prior DFT study of *trans*/*cis* equilibria for a *series* of bis(phosphine) complexes $PtCl_2L_2$, although data for some individual complexes exist [25].

Only in rare cases have we been able to obtain crystal structures of the various metathesis precursors in Scheme 1 [3b,4d,12b,13]. Although these do not have a direct relationship to reactivity or product selectivities, they nonetheless can help to visualize various outcomes. In the case of *cis*-**5** (Fig. 2, top), it can be immediately appreciated that if the two $(CH_2)_6CH{=}CH_2$ moieties whose termini are most proximal undergo ring closing metathesis (C8_2 and C8_5), the system becomes "locked in" to deliver a product in which the two phenyl rings are *syn*.

In summary, the results reported in this paper break new ground in terms rotator/stator interactions that can be used to modulate rotational barriers, and augment previous observations regarding *trans*/*cis* and *syn*/*anti* selectivities in the types of ring closing metatheses highlighted in Scheme 1, as well as the precursor complexes. Additional studies related to these themes, as well as properties of the free diphosphine ligands that can be liberated from some of these species [26], will be reported in due course.

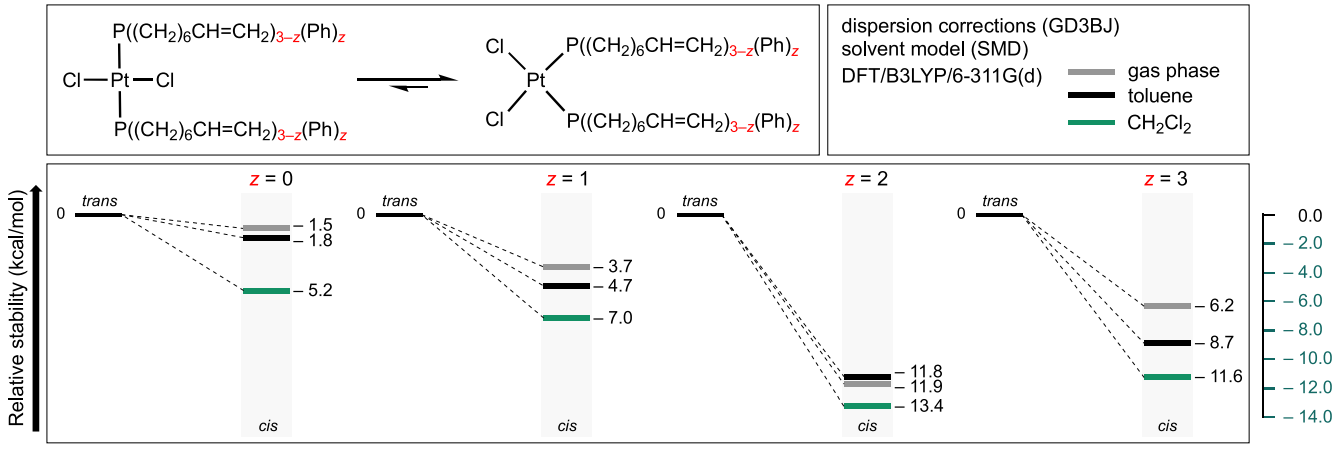

Fig. 3. Relative energies (kcal/mol) of *trans* and *cis* bis(phosphine) platinum dichloride complexes as computed by DFT (for ease of comparison, the energies of the *trans* isomers are set to 0 in all media).

4. Experimental

4.1. General

General procedures involving inert atmospheres and instrumentation were identical with those given in recent papers [6c,12b]. Chemicals were treated as follows: toluene and THF, distilled from Na/benzophenone or purified using a Glass Contour system; CH_2Cl_2, used as received (chromatographies) or purified using a Glass Contour system; $CDCl_3$ distilled from CaH_2; Grubbs' first generation catalyst ($(Cy_3P)_2RuCl_2(=CHPh)$), Wilkinson's catalyst ($RhCl(PPh_3)_3$), PtO_2, $PtCl_2$, C_6D_6, diethyl ether, and acetone, used as received from common commercial suppliers.

4.2. *trans*-$PtCl_2(P(OH)((CH_2)_6CH{=}CH_2)_2)_2$ (*trans*-**2**)

A Schlenk flask was charged with $PtCl_2$ (0.2591 g, 0.974 mmol), (O=)$PH((CH_2)_6CH{=}CH_2)_2$ (**1** [13]; 0.5262 g, 1.946 mmol), and toluene (20 mL) with stirring. After 5 d, the mixture was concentrated to ca. 2 mL and placed at the top of a silica column (3.5 × 20 cm), which was eluted with hexanes/CH_2Cl_2 (60:40 to 80:20 v/v) and then CH_2Cl_2. The solvent was removed from the product fractions by oil pump vacuum to give *trans*-**2** as a pale yellow oil (0.5342 g, 0.662 mmol, 68%) and a ca. 82:18 mixture of *anti*/*syn* isomers.[9]

NMR (/ppm, $CDCl_3$)[9]: ^{1}H (500MHz) 5.80 (ddt, 4H, $^3J_{HHtrans}$=17.0 Hz, $^3J_{HHcis}$=10.1Hz, $^3J_{HH}$=6.7Hz, C*H*=), 5.45 (br s, 2H, O*H*), 4.99 (br d, 4H, $^3J_{HHtrans}$=17.1Hz, =CH_EH_Z), 4.93 (br d, 4H, $^3J_{HHcis}$=10.3Hz, =CH_EH_Z), 2.111.76 (m, 20H, CH_2CH=, CH_2), 1.721.61 (m, 4H, CH_2), 1.511.30 (br m, 24H, remaining CH_2); ^{13}C{^{1}H} (126MHz) 139.0 (s, *C*H=, *anti*), 138.6 (s, *C*H=, *syn*), 114.5 (s, =CH_2, *syn*), 114.3 (s, =CH_2, *anti*), 33.72 (s, CH_2*C*H=, *anti*), 33.70 (s, CH_2*C*H=, *syn*), 30.9 (s, CH_2, *syn*), 30.7 (s, CH_2, *anti*), 30.5 (t, $^3J_{CP}$=6.7Hz, PCH_2CH_2CH_2, *anti*+*syn*), 28.9 (s, CH_2, *syn*), 28.8 (s, CH_2, *anti*), 28.7 (s, CH_2, *anti*+*syn*), 23.1 (s, CH_2, *anti*), 23.0 (s, CH_2, *syn*); ^{31}P{^{1}H} (202MHz) 105.0 (s, $^1J_{PPt}$=2391Hz, 18%, *syn*),[10] 103.4 (s, $^1J_{PPt}$=2387Hz, 82%, *anti*).[10]

4.3. *trans*-$\overline{PtCl_2(P(OH)((CH_2)_{14})_2P(OH))}$ (*trans*-**3**)

A. A two necked flask was charged with a solution of *trans*-**2** (0.356 g, 0.441 mmol; crude[9b]) in CH_2Cl_2 (126 mL; 0.0035 M in *trans*-**2**) and cooled to 0 °C. A solution of Grubbs' first generation catalyst (0.011 g, 0.013 mmol, 2.9 mol%) in CH_2Cl_2 (44 mL) was added dropwise with stirring. A precipitate gradually formed. After 39 h, the mixture was filtered and the filtrate concentrated to 30 mL by rotary evaporation (weight of solid removed: 0.139 g). A Fischer-Porter bottle was charged with the concentrated filtrate (estimated loading of soluble metathesis product: 0.192 g, 0.256 mmol) and $RhCl(PPh_3)_3$ (0.060 g, 0.065 mmol, 25 mol%), flushed with H_2, and pressurized to 5 bar of H_2. The solution was stirred at 38 °C for 18 h and then passed through Celatom. The filter cake was washed with CH_2Cl_2 (3 × 5 mL). The solvent was removed from the combined organic phases by rotary evaporation. The residue was chromatographed on a silica column (1:2 v/v acetone/CH_2Cl_2). The product fraction was passed through a silica pad (Ø 4 × 2.5 cm) and the solvent removed by rotary evaporation to give *trans*-**3** as a pale yellow, slowly solidifying oil (0.104 g, 0.138 mmol, 31%).

^{31}P{^{1}H} NMR (122 MHz, δ/ppm, C_6D_6) 106.5 (*trans*-**3**, s, $^1J_{PPt}$ = 2473 Hz, 83%),[10] 105.4 (s, 17%).[11]

B. A three necked flask was charged with solutions of *trans*-**2** (0.3324 g, 0.412 mmol) in CH_2Cl_2 (500 mL; 0.00082 M in *trans*-**2**) and Grubbs' first generation catalyst (0.022 g, 0.027 mmol; 6.6 mol%) in CH_2Cl_2 (10 mL), and fitted with a condenser. The solution was refluxed with stirring and a precipitate began to form. After 48 h, the mixture was cooled and the solvent was removed by oil pump vacuum. Some CH_2Cl_2 was added, and the sample was passed through a short neutral alumina pad, rinsing with acetone/CH_2Cl_2 (1:1 v/v). The solvent was removed from the combined organic phases by rotary evaporation. A Fischer-Porter bottle was charged with the residue, CH_2Cl_2 (20 mL), PtO_2 (0.0162 g, 0.0714 mmol, 17 mol%), and H_2 (5 bar). The mixture was stirred at 50 °C (venting H_2 to maintain 5 bar) for 48 h and cooled. The solvent removed by oil pump vacuum. The residue was placed at the top of a silica column (Ø 2.5 × 14 cm), which was eluted with acetone/CH_2Cl_2 (1:2 v/v). The solvent was removed from the product fractions by rotary evaporation to give *trans*-**3** (0.0287 g, 0.038 mmol, 9%) as a pale yellow, slowly solidifying oil.

NMR (δ/ppm, C_6D_6): ^{1}H (500 MHz) 2.07–1.96 (m, 8H, CH_2), 1.87–1.75 (m, 8H, CH_2), 1.74–1.62 (m, 8H, CH_2), 1.46–1.31 (m, 32H, remaining CH_2); ^{13}C{^{1}H} (126 MHz) 30.6 (t, J_{CP} = 20.9 Hz, CH_2), 30.4 (t, J_{CP} = 6.6 Hz, CH_2), 28.3 (s, CH_2), 27.7 (s, CH_2), 27.1 (s, CH_2), 26.3 (s, CH_2), 23.7 (s, CH_2); ^{31}P{^{1}H} (202 MHz) 106.5 (*trans*-**3**, s, $^1J_{PPt}$ = 2471 Hz, 84%),[10] 105.44 (s, 8%),[11] 105.36 (s, 8%).[11] IR (cm^{-1}, powder film, ATR): 3302 (br, PO-H), 2916 (s), 2854 (m), 1257 (s), 1088 (s), 1018 (s), 864 (s), 794 (s), 710 (w).

C. Colorless needles of *trans*-**3** were obtained by the vapor diffusion of diethyl ether into CH_2Cl_2 solutions of the preceding samples at room temperature.

4.4. $PtCl_2(P(Ph)((CH_2)_6CH{=}CH_2)_2)_2$ (**5**)

A suspension of $PtCl_2$ (2.295 g, 8.628 mmol) in toluene (50 mL) was cooled to 0 °C. A solution of $P(Ph)((CH_2)_6CH{=}CH_2)_2$ (**4** [4b]; 5.592 g, 16.920 mmol) in toluene (20 mL) was added dropwise with stirring over 20 min. The mixture was stirred overnight, concentrated to ca. 5 mL, and placed at the top of an alumina column (Ø 8.5 × 16 cm), which was eluted with CH_2Cl_2. The solvent was removed from the product containing fractions to give *trans*-**5** as a yellow oil (0.649 g, 0.700 mmol, 8% with up to 10% *cis*-**5**) and *cis*-**5** as a colorless solid (3.122 g, 3.368 mmol, 40%). Colorless plates of *cis*-**5** were obtained by the slow evaporative concentration of diethyl ether solutions at room temperature.

Data for *trans*-**5**. NMR (δ/ppm, $CDCl_3$): ^{1}H (300 MHz) 7.73–7.67, 7.39–7.37 (2 × m, 10H, Ph), 5.87–5.70 (m, 4H, C*H*=CH_2), 5.01–4.88 (m, 8H, =CH_2), 2.06–1.96 (m, 8H, PCH_2), 1.64–1.24 (m, 40H, remaining CH_2); ^{13}C{^{1}H} (75 MHz) 139.0 (s, *C*H=CH_2), 132.2 (virtual t, J_{CP} = 5.5 Hz, *o*-Ph) [27], 130.0 (s, Ph), 128.2 (virtual t, J_{CP} = 4.9 Hz, *m*-Ph) [27], 114.3 (s, =CH_2), 33.7 (s, CH_2*C*H=), 31.0 (virtual t, J_{CP} = 7.0 Hz, PCH_2CH_2CH_2) [27], 28.7, 28.6, 23.4 (3 × s, CH_2), 20.9 (virtual t, J_{CP} = 16.8 Hz, PCH_2) [27]; ^{31}P{^{1}H} (122 MHz) 7.1 (s, $^1J_{PPt}$ = 2462 Hz).[10]

Data for *cis*-**5**. Elemental analysis calcd (%) for $C_{44}H_{70}Cl_2P_2Pt$: C 57.01, H 7.61, Cl 7.65; found: C 56.95, H 7.65, Cl 7.65. NMR (δ/ppm): ^{1}H (300 MHz, $CDCl_3$) 7.44–7.39, 7.31–7.21 (2 × m, 10H, Ph), 5.82–5.69 (m, 4H, C*H*=CH_2), 4.99–4.90 (m, 8H, =CH_2), 2.02–1.95 (m, 16H, CH_2), 1.45–1.22 (m, 48H, CH_2); ^{13}C{^{1}H} (75 MHz,

[9] (a) The *anti*/*syn* isomer assignments for *trans*-**2** are based upon the very similar ratios and NMR properties found for *anti*/*syn* *cis*-$PtCl_2(P(OH)(t\text{-}Bu)_2)_2$ [20]. (b) When the workup is shortened to a simple filtration and toluene extraction of the filter cake, an additional ^{31}P{^{1}H} NMR signal is observed (δ/ppm, toluene, 162 MHz) at 64.0 ppm (s, $^1J_{PPt}$ = 3969 Hz, ca. 15%).[10] This may be a *cis*,*cis* diplatinum species as shown in Fig. 4 of Ref. [20].

[10] This coupling represents a satellite (d, ^{195}Pt=33.8%), and is not reflected in the peak multiplicity given.

[11] For this less intense signal, ^{195}Pt satellites could not be detected. For possible assignments, see the text.

C_6D_6) 138.8 (s, *C*H=CH_2), 131.4 (virtual t, J_{CP} = 4.3 Hz, *o*-Ph) [27], 130.8 (s, Ph), 128.4 (virtual t, J_{CP} = 4.8 Hz, *m*-Ph) [27], 114.3 (s, =CH_2), 33.6 (s, CH_2CH=), 30.6 (virtual t, J_{CP} = 7.5 Hz, $PCH_2CH_2CH_2$) [27], 28.6 (s, CH_2), 28.5 (s, CH_2), 23.8, 23.6 (s and obscured virtual t, CH_2 and PCH_2); $^{31}P\{^1H\}$ (122 MHz, C_6D_6) −1.9 (s, $^1J_{PPt}$ = 3550 Hz).[10] MS (ESI+, *m*/*z*) 891.6 ([M–Cl]$^+$, 86%).

4.5. Crystallization of *cis*-$PtCl_2((H_2C)_{14}P((CH_2)_{14})P(CH_2)_{14})$ (*cis*-**7′**)

A diethyl ether solution of *trans*-**7′** [6b] was allowed to slowly concentrate for several months at room temperature. Colorless plates and a yellow oil resulted. The former were collected and shown by X-ray crystallography (below) to be *cis*-**7′**. A $^{13}C\{^1H\}$ NMR spectrum showed the oil to be *trans*-**7′**. Elemental analysis calcd (%) for $C_{42}H_{84}P_2PtCl_2$: C 55.01, H 9.23; found: C 55.13, H 9.45. $^{31}P\{^1H\}$ NMR (202 MHz, δ/ppm, $CDCl_3$): 2.2 (s, $^1J_{PPt}$ = 3522 Hz).[10]

4.6. Crystallography

Samples were crystallized as described above and data were collected as outlined in Table 1. **A.** The cell parameters of *trans*-**3** were obtained from 2500 data frames using ω and φ scans and refined with 14524 reflections. Integrated intensity information for each reflection was obtained by reduction of the data frames with SAINT [28]. Lorentz and polarization corrections were applied, data were scaled, and absorption corrections were applied using SADABS [29]. Employing Olex2 [30], the structure was solved by direct methods using SHELXT [31] and refined (weighted least squares refinement on F^2) using SHELXL [31]. Non-hydrogen atoms were refined with anisotropic thermal parameters. The O—H hydrogen atoms were located in an electron density map and the O—H distances fixed. Other hydrogen atoms were placed in idealized positions. Both sets were refined using a riding model. The molecular structure exhibited an inversion center at platinum. **B.** The structure of *cis*-**5** was solved as in A (31387 reflections). One eight carbon segment was disordered (C1_5 to C8_5). This could be modeled by invoking two positions with an occupancy ratio of 52:48. A combination of SHELXL SADI restraints were applied to the geometries of these carbon atoms, which were refined anisotropically to convergence. **C**. The cell parameters of *trans*-**7′** were obtained from 180 data frames using a 0.5° scan and refined with 39,125 reflections using SAINT [28]. Integrated intensity information for each reflection was obtained by reduction of the data frames with APEX2 [32]. Additional steps were carried out as in A. A large electron density peak (ca. 10 e$Å^{-3}$) was observed 1.6 Å from Cl1, and many of the thermal ellipsoids of the methylene carbon atoms were elongated. Efforts to model this disorder not only increased the number of parameters, but also did not improve the reliability factors. Accordingly, strong restraints (SIMU and DELU) were used to keep the thermal ellipsoids meaningful.

4.7. Computational data

Computations were performed with the Gaussian 09 package [33], employing the ultrafine grid (99,590) to enhance accuracy. Geometries were optimized using density functional theory (DFT) in the gas phase. The B3LYP functional [34–36] was employed with an all-electron 6-311+G(d) [37] basis set on all atoms except platinum, which was treated using an effective core potential (ECP60MDF) [38] and the cc-pVTZ-PP [38] basis set. The optimized structures were subjected to frequency calculations (using the same functional and basis set as above) to confirm that all structures were local minima. Solvent corrections using the SMD model as single point calculations were carried out for toluene and dichloromethane [39]. Dispersion corrections were implemented for all calculations using the D3 version of Grimme's dispersion function with Becke-Johnson damping (referred to as GD3BJ) [40]. The structures of the calculated species are disclosed in xyz formatted text files (Supporting Information File 1) that can be opened with a variety of programs, e.g. Mercury [41]; they contain the optimized geometries of all computed structures [42].

Acknowledgements

The authors thank the US National Science Foundation (CHE-1566601 and CHE-1664866) for support, the Laboratory for Molecular Simulation and Texas A&M High Performance Research Computing Facility for computational resources, and Dr. Lisa M. Pérez (Laboratory for Molecular Simulation) for helpful discussions.

Notes

The authors declare no competing financial interest.

Appendix A. Supplementary data

CCDC 1852571, 1852572, and 1852573 contains the supplementary crystallographic data for *trans*-**3**, *cis*-**5**, and *cis*-**7′**. These data can be obtained free of charge via http://www.ccdc.cam.ac.uk/conts/retrieving.html, or from the Cambridge Crystallographic Data Centre, 12 Union Road, Cambridge CB2 1EZ, UK; fax: (+44) 1223-336-033; or e-mail: deposit@ccdc.cam.ac.uk. Supplementary data to this article can be found online at https://doi.org/10.1016/j.poly.2018.09.025.

References

[1] Review: T. Fiedler, J.A. Gladysz, Multifold ring closing olefin metatheses in syntheses of organometallic molecules with unusual connectivities, in: K. Grela (Ed.), Olefin Metathesis – Theory and Practice, John Wiley & Sons, Hoboken, New Jersey, 2014, p. 311.
[2] Recent examples from the year 2018: (a) L. Zhang, D.P. August, J. Zhong, G.F.S. Whitehead, I.J. Vitorica-Yrezabal, D.A. Leigh, J. Am. Chem. Soc. 140 (2018) 4982;
(b) H. Takashima, Y. Inagaki, H. Momma, E. Kwon, K. Yamaguchi, W. Setaka, Organometallics 37 (2018) 1501.
[3] (a) E.B. Bauer, F. Hampel, J.A. Gladysz, Organometallics 22 (2003) 5567;
(b) N. Lewanzik, T. Oeser, J. Blümel, J.A. Gladysz, J. Mol. Catal. A 254 (2006) 20.
[4] (a) T. Shima, E.B. Bauer, F. Hampel, J.A. Gladysz, Dalton Trans. 33 (2004) 1012;
(b) E. Steigleder, T. Shima, G.M. Lang, A. Ehnbom, F. Hampel, J.A. Gladysz, Organometallics 36 (2017) 2891;
(c) , Analogs of **IV** featuring selenium donor ligands:H. Joshi, S. Kharel, N. Bhuvanesh, J.A. Gladysz J. Organomet. Chem. 875 (2018) 80;
(d) , Analogs of **IV** featuring pyridine donor ligands:P.D. Zeits, G.P. Rachiero, F. Hampel, J.H. Reibenspies, J.A. Gladysz Organometallics 31 (2012) 2854.
[5] (a) T. Shima, F. Hampel, J.A. Gladysz, Angew. Chem., Int. Ed. 43 (2004) 5537, Angew. Chem. 116 (2004) 5653;
(b) G.M. Lang, T. Shima, L. Wang, K.J. Cluff, F. Hampel, J. Blümel, J.A. Gladysz, J. Am. Chem. Soc. 138 (2016) 7649;
(c) G.M. Lang, N. Bhuvanesh, J.H. Reibenspies, J.A. Gladysz, Organometallics 35 (2016) 2873;
(d) G.M. Lang, D. Skaper, F. Hampel, J.A. Gladysz, Dalton Trans. 45 (2016) 16190.
[6] (a) A.J. Nawara, T. Shima, F. Hampel, J.A. Gladysz, J. Am. Chem. Soc. 128 (2006) 4962;
(b) A.J. Nawara-Hultzsch, M. Stollenz, M. Barbasiewicz, S. Szafert, T. Lis, F. Hampel, N. Bhuvanesh, J.A. Gladysz, Chem. Eur. J. 20 (2014) 4617;
(c) H. Joshi, S. Kharel, N. Bhuvanesh, J.A. Gladysz, Organometallics 37 (2018) 2991.
[7] (a) L. Wang, F. Hampel, J.A. Gladysz, Angew. Chem., Int. Ed. 45 (2006) 4372, Angew. Chem. 118 (2006) 4479;
(b) L. Wang, T. Shima, F. Hampel, J.A. Gladysz, Chem. Commun. (2006) 4075;
(c) A.L. Estrada, T. Jia, N. Bhuvanesh, J. Blümel, J.A. Gladysz, Eur. J. Inorg. Chem. 2015 (2015) 5318.
[8] (a) T. Fiedler, N. Bhuvanesh, F. Hampel, J.H. Reibenspies, J.A. Gladysz, Dalton Trans. 45 (2016) 7131;
(b) G.D. Hess, T. Fiedler, F. Hampel, J.A. Gladysz, Inorg. Chem. 56 (2017) 7454.
[9] G.S. Kottas, L.I. Clarke, D. Horinek, J. Michl, Chem. Rev. 105 (2005) 1281.
[10] C.S. Vogelsberg, M.A. Garcia-Garibay, Chem. Soc. Rev. 41 (2012) 1892.
[11] M. Tsurunaga, Y. Inagaki, H. Momma, E. Kwon, K. Yamaguchi, K. Yoza, W. Setaka, submitted for publication, and earlier work from this group cited therein.

[12] (a) K. Skopek, M. Barbasiewicz, F. Hampel, J.A. Gladysz, Inorg. Chem. 47 (2008) 3474;
(b) H. Joshi, S. Kharel, A. Ehnbom, K. Skopek, G.D. Hess, T. Fiedler, F. Hampel, N. Bhuvanesh, J.A. Gladysz, J. Am. Chem. Soc. 140 (2018) 8463.
[13] S. Kharel, T. Jia, N. Bhuvanesh, J.H. Reibenspies, J. Blümel, J.A. Gladysz, Chem. Asian J. 13 (2018) 2632.
[14] (a) W.J. Pietro, W.J. Hehre, J. Am. Chem. Soc. 104 (1982) 3594;
(b) H.I. Kenttämaa, R.G. Cooks, J. Am. Chem. Soc. 107 (1985) 1881.
[15] Reviews of older literature: (a) D.M. Roundhill, R.P. Sperline, W.B. Beaulieu, Coord. Chem. Rev. 26 (1978) 263;
(b) B. Walther, Coord. Chem. Rev. 60 (1984) 67.
[16] (a) S.O. Grim, R.L. Keiter, W. McFarlane, Inorg. Chem. 6 (1967) 1133;
(b) C.J. Cobley, P.G. Pringle, Inorg. Chim. Acta 265 (1997) 107.
[17] A.J. Nawara-Hultzsch, K. Skopek, T. Shima, M. Barbasiewicz, G.D. Hess, D. Skaper, J.A. Gladysz, Z. Naturforsch. B: Anorg. Chem., Org. Chem. 65 (2010) 414.
[18] F.R. Hartley, Organometal. Chem. Rev. A 6 (1970) 119.
[19] B. Kurscheid, B. Neumann, H.-G. Stammler, B. Hoge, Chem. Eur. J. 17 (2011) 14935.
[20] T. Achard, L. Giordano, A. Tenaglia, Y. Gimbert, G. Buono, Organometallics 29 (2010) 3936.
[21] T.-W. Chang, P.-Y. Ho, K.-C. Mao, F.-E. Hong, Dalton Trans. 44 (2015) 17129.
[22] (a) R.D. Gillard, M.F. Pilbrow, J. Chem. Soc., Dalton Trans. (1974) 2320;
(b) B. Cavinato, L. Toniolo, Inorg. Chim. Acta 52 (1981) 39;
(c) L. Rigamonti, C. Manassero, M. Rusconi, M. Manassero, A. Pasini, Dalton Trans. 1974 (2009) 1206.
[23] (a) C.A. Tolman, Chem. Rev. 77 (1977) 313 (see also Appendix A);
(b) C.H. Suresh, N. Koga, Inorg. Chem. 41 (2002) 1573.
[24] H. Brunner, T. Tsuno, Inorg. Chim. Acta 446 (2016) 132.
[25] (a) C. Hansson, S. Carlson, D. Giveen, M. Johansson, S. Yong, Å. Oskarsson, Acta Cryst. B62 (2006) 474;
(b) Z. Kokan, B. Perić, G. Kovačević, A. Brozovic, N. Metzler-Nolte, S.I. Kirin, Eur. J. Inorg. Chem. 2017 (2017) 3928.
[26] (a) M. Stollenz, M. Barbasiewicz, A.J. Nawara-Hultzsch, T. Fiedler, R.M. Laddusaw, N. Bhuvanesh, J.A. Gladysz, Angew. Chem., Int. Ed. 50 (2011) 6647, Angew. Chem. 123 (2011) 6777;
(b) S. Kharel, H. Joshi, S. Bierschenk, M. Stollenz, D. Taher, N. Bhuvanesh, J.A. Gladysz, J. Am. Chem. Soc. 139 (2017) 2172.
[27] W.H. Hersh, J. Chem. Educ. 74 (1997) 1485.
[28] FRAMBO/SAINT, Bruker AXS Inc., Madison, WI, USA, 2001.
[29] Sheldrick, G. M. SADABS, Bruker AXS Inc., Madison, WI, USA, 2001.
[30] O.V. Dolomanov, L.J. Bourhis, R.J. Gildea, J.A.K. Howard, H.J. Puschmann, Appl. Cryst. 42 (2009) 339.
[31] (a) G.M. Sheldrick, Acta Cryst. A64 (2008) 112;
(b) G.M. Sheldrick, Acta Cryst. A71 (2015) 3;
(c) G.M. Sheldrick, Acta Cryst. C71 (2015) 3.
[32] APEX2, Bruker AXS Inc., Madison, WI, USA, 2012.
[33] M.J.G.W. Frisch, H.B. Trucks, G.E. Schlegel, M.A. Scuseria, J.R. Robb, G. Cheeseman, V. Scalmani, B. Barone, G.A. Mennucci, H. Petersson, M. Nakatsuji, X. Caricato, H.P. Li, A.F. Hratchian, J. Izmaylov, G. Bloino, J.L. Zheng, M. Sonnenberg, M. Hada, K. Ehara, R. Toyota, J. Fukuda, M. Hasegawa, T. Ishida, Y. Nakajima, O. Honda, H. Kitao, T. Nakai, J.A. Vreven, Jr. Montgomery, J. E. Peralta, F. Ogliaro, M. Bearpark, J.J. Heyd, E. Brothers, K.N. Kudin, V.N. Staroverov, R. Kobayashi, J. Normand, K. Raghavachari, A. Rendell, J.C. Burant, S.S. Iyengar, J. Tomasi, M. Cossi, N. Rega, J.M. Millam, M. Klene, J.E. Knox, J.B. Cross, V. Bakken, C. Adamo, J. Jaramillo, R. Gomperts, R.E. Stratmann, O. Yazyev, A.J. Austin, R. Cammi, C. Pomelli, J.W. Ochterski, R.L. Martin, K. Morokuma, V.G. Zakrzewski, G.A. Voth, P. Salvador, J.J. Dannenberg, S. Dapprich, A.D. Daniels, Ö. Farkas, J.B. Foresman, J.V. Ortiz, J. Cioslowski, D.J. Fox, Gaussian 09, Revision D.01, Gaussian Inc, Wallingford, CT, USA, 2009.
[34] A.D. Becke, Phys. Rev. A 38 (1988) 3098.
[35] A.D. Becke, J. Chem. Phys. 98 (1993) 5648.
[36] C. Lee, W. Yang, R.G. Parr, Phys. Rev. B 37 (1988) 785.
[37] P.C. Hariharan, J.A. Pople, Theor. Chim. Acta 28 (1973) 213.
[38] D. Figgen, K.A. Peterson, M. Dolg, H. Stoll, J. Chem. Phys. 130 (2009) 164108.
[39] A.V. Marenich, C.J. Cramer, D.G. Truhlar, J. Phys. Chem. B 113 (2009) 6378.
[40] S. Grimme, S. Ehrlich, L. Goerigk, J. Comput. Chem. 32 (2011) 1456.
[41] C.F. Macrae, I.J. Bruno, J.A. Chisholm, P.R. Edgington, P. McCabe, E. Pidcock, L. Rodriguez-Monge, R. Taylor, J. van de Streek, P.A. Wood, J. Appl. Crystallogr. 41 (2008) 466.
[42] D.L. Lichtenberger, J.A. Gladysz, Organometallics 33 (2014) 835.